Aalborg Universitet

AALBORG UNIVERSITY
DENMARK

Robust MPC-based Current Controller against Grid Impedance Variations for Single-Phase Grid-Connected Inverters

 Zangeneh Bighash, Esmaeil; Sadeghzadeh, Seyed Mohammad ; Ebrahimzadeh, Esmaeil; Blaabjerg, Frede

Accepted Manuscript

Robust MPC-based current controller against grid impedance variation for single-phase grid-connected inverters

Esmaeil Zangeneh Bighash, Seyed Mohammad Sadeghzadeh, Esmaeil Ebrahimzade, Frede Blaabjerg
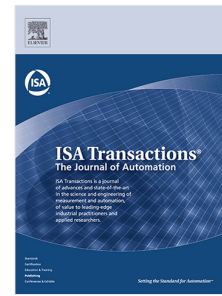
Please cite this article as: E. Zangeneh Bighash, et al. Robust MPC-based current controller against grid impedance variation for single-phase grid-connected inverters. *ISA Transactions* (2018), https://doi.org/10.1016/j.isatra.2018.09.021

- An MPC-based current controlled for single phase grid connected inverters has been proposed.

- The grid impedance variation and its effect on resonance of LCL filters has been discussed.

- The results of the proposed controller have been compared with a classical PR controller.

- The results showed that the proposed MPC method, in contrast with the PR controller, is robust when grid impedance changes.

Robust MPC-based Current Controller against Grid Impedance Variations for Single-Phase Grid-Connected Inverters

Esmaeil Zangeneh Bighash, Seyed Mohammad Sadeghzadeh, Esmaeil Ebrahimzadeh, and Frede Blaabjerg

Esmaeil	Zangeneh Bighash	PHD Student	Faculty of Electrical Engineering Shahed University, Tehran	esmaeilzangane@gmail.com
Seyed Mohammad	Sadeghzadeh	Associate Professor	Faculty of Engineering, Shahed University, Tehran	sm.sadeghzadeh@gmail.com
Esmaeil	Ebrahimzade	PHD Student	Energy Department, Aalborg University, Aalborg	ebb@et.aau.dk
Frede	Blaabjerg	Professor	Energy Department, Aalborg University, Aalborg	fbl@et.aau.dk

Robust MPC-based Current Controller against Grid Impedance Variation for Single-Phase Grid-Connected Inverters

Abstract- Recently, LCL filters have been widely used in the output of single phase inverters. Since, the grid side inductor in these filters is in series with the grid impedance at the Point of Common Coupling (PCC), it may create new resonances. This phenomena may take the control loop toward instability. In this case, in order to have a reliable operation, the current controller should be insensitive to the grid impedance variation. In order to damp these resonances, researchers have presented some methods using active or passive damping. These methods added an extra loop to the control loop, an extra passive component in the filter or extra sensor in the control process. But in most of them, the complexity and the cost of controller have been increased. Therefore, presenting a simple control method without extra sensor, passive component or extra arrangement can be a promising approach. This paper presents an MPC-based current controller, which is simple and robust against the grid impedance variation and even the variation of the LCL filter parameters. In contrast to classical multi-loop controller like Proportional-Resonant (PR) controllers, the proposed control method does not need any parameter tuning. In the proposed controller, the switching plan and duty cycles are determined by a cost function and a switching table. Therefore, at the same time with any variation in grid impedance, the proposed controller changes the next switching state and duty cycle. Operating performance like look-up table, searching in all possible switching states to find the best state for the next switching period, makes the controller adaptive and robust against the variation of LCL filter parameters. In order to confirm the effectiveness of the proposed controller, simulations and experimental results of the proposed controller are compared with a classical PR controller.

Keywords: Model Predictive Current Controller (MPCC), Grid-connected inverters, Grid impedance variation, Inductor-capacitor-inductor (LCL) filter, Proportional-Resonant (PR) controller.

I. INTRODUCTION

Recently, instead of the L filters, the LCL filters are widely used in the output of single phase grid-connected inverters. [1-2]. These filters have more advantages against the L type filters, they can attenuate higher-frequency harmonics and also make the inverter operate in both stand-alone and grid-connected condition. However, the resonance phenomena in these filters can create some instability concern [3-5]. Therefore, preventing the resonance phenomena in these filters has involved the researchers to work on it. In this case, some studies introduced some solutions. Authors

in [6] surveyed the impact of controller bandwidth on the filter resonance frequency. The results show the control frequency, as far as possible, should be lower than the resonance frequency of the filter. In the following, in [7-8], a trade-off between the control frequency and filter resonance frequency is considered to have an appropriate design for these filters. But, in spite of an appropriate design for the LCL filter, due to grid impedance variation in series with the grid side filter inductor, the resonance frequency can change during control process and this variation can goes the inverter control loop toward instability [9]. Therefore, In order to address this challenge, the controller should online damp the resonance frequency during the control process. In this case, some approaches have been presented. For example, in [10]-[12], notch filters are used before the modulation part, in order to filter the determined inverter voltage reference at the resonance frequency. In this method, by online estimating the grid impedance, the resonance frequency for the LCL filter is calculated and used for tuning the notch filter. In [13], authors proposed a robust H∞ controller to make robust the control loop against the grid impedance variation by adding an extra loop in the control loop. In this approach, controller exhibits high gains around the fundamental frequency, similar to the traditional proportional-resonant (PR) controller. In [14], a wide damping region for the LCL filter is proposed by adding a capacitor current feedback to the control loop. Although all aforementioned control methods have robust and acceptable performance in suppression the resonance, but in these approaches, the controllers are forced to use more sensors or their performance are depend on processing some online condition for online-gain tuning in the control loop. Therefore, they made the controllers costly and complex. In this regard, a control system can be more attractive which no need to have an additional sensor or complex computing for control loop. Recently, due to progress in the industrial processors, researches on model predictive controller have been a hot field. Model predictive controllers have fast response, light computational and, easy implementation. These controllers are based on a cost function and can simultaneously track multi-object in control [15-16]. Therefore, the proposed controller in this paper is based on a model predictive controller (MPC) named model predictive current controller (MPCC). The proposed method does not require any parameter tuning and it is not sensitive to the grid impedance variation. In the proposed approach, the control scheme is based on a cost function and a switching table with some virtual vectors. Because of having a processing property like look-up table process, the proposed controller adaptively changes the switching plan and duty cycle in each switching period when the grid impedance changes. Simulation an experimental results will show the performance of proposed controller. As it is mentioned, in order to prove the performance of the proposed controller against the grid impedance variation, the simulation and experimental results are compared with a classical PR controller.

The paper is organized as follow: first, the proposed method is introduced in section II; next, the robustness of the proposed controller is discussed in section III; then, simulation and experimental results of the proposed controller are compared with the classical PR controller in section IV; and finally, the conclusion part is discussed in section VI.

II. THE PROPOSED ROBUST MODEL PREDICTIVE CONTROL

A. Principle of MPCC

Model predictive control design and implementation consist of the following three steps:

- Using a model to predict the behavior of control variables for the next step time.
- Determining a cost function includes control objectives and expected behavior of the system.
- Extract the appropriate command to minimize the cost function value.

B. Modeling of the power stage

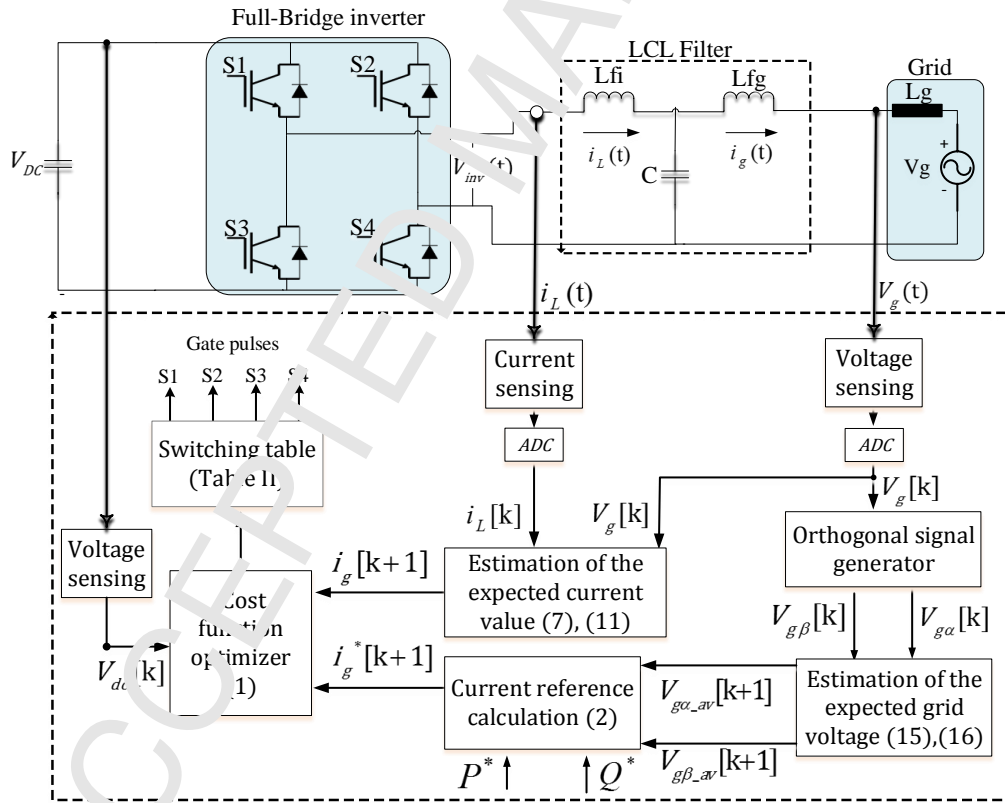Block diagram of the proposed MPCC method is given in Fig. 1.

Fig. 1. Proposed MPCC control block diagram for single phase inverter.

In order to track clearly the equations in the paper, the parameters have been named and listed as Table. I.

TABLE I
Parameter definition

L_{fi}	Inverter side inductor
L_{fg}	Grid side inductor
C	LCL capacitor
$V_g(t)$	Grid voltage
$V_{inv}(t)$	Inverter output voltage
$V_{dc}(t)$	Dc-link voltage
g	Cost function
$i_g{}^*[k+1]$	Current reference (for the next switching period)
$i_g[k+1]$	Predicted current (for the next switching period)
$V_{g\_av}[k]$	The average of grid voltage over one sampling period
$V_{g\_av}[k+1]$	The average of grid voltage over one sampling period (for the next switching period)
$V_{g\alpha\_av}[k+1]$	The average of grid voltage over one sampling period (for the next switching period in α frame)
$V_{g\beta\_av}[k+1]$	The average of grid voltage over one sampling period (for the switching period in β frame)
$V_{inv\_av}[k]$ or $V_{inv}[k]^*$	The average of inverter voltage selected by cost function as inverter voltage reference
(S_a, S_b)	Switching states
T_s	Switching time
T_d	Duty cycle time
T_j	Zero cycle time
n	The number of vectors

1) The proposed MPCC controller

In the proposed controller, the grid current reference for the next sample will be determined and the predicted current is calculated from the system model. Finally, the grid current is controlled by a cost function as

$$g = \left| i_g{}^*[k+1] - i_g[k+1] \right| \qquad (1)$$

where $i_g{}^*[k+1]$ is the next sample of the grid current reference and $i_g[k+1]$ is calculated and predicted by the system model, which is presented in the next sections.

2) Calculation of the grid current reference ($i_g{}^*[k+1]$)

The current reference to achieve P* and Q* is determined from (2).

$$i_g{}^*[k+1] = \frac{2}{V_{g\alpha\_av}[k+1]^2 + V_{g\beta\_av}[k+1]^2} \left[V_{g\alpha\_av}[k+1] \quad V_{g\beta\_av}[k+1] \right] \begin{bmatrix} P^* \\ Q^* \end{bmatrix} \quad (2)$$

where $V_{g\alpha\_av}[k+1]$ and $V_{g\beta\_av}[k+1]$ are the average of orthogonal components for the grid voltage, which are calculated by (15) and (16).

3) Calculation of the estimated current ($i_g[k+1]$)

In order to calculate $i_g[k+1]$, the inverter can be modeled by the following.

$$V_{inv}(t) = L_{fi} \frac{di_L(t)}{dt} + V_c(t) \quad (3)$$

where

$$V_c(t) = V_g(t) + L_{fg} \frac{di_g(t)}{dt} \quad (4)$$

Substituting (4) in (3)

$$V_{inv}(t) = V_g(t) + L_{fi} \frac{di_L(t)}{dt} + L_{fg} \frac{di_g(t)}{dt} \quad (5)$$

Assuming that the inverter works with a fixed frequency, the switching time is constant, T_s. Rewrite (5) in discrete-time shape and employing the Euler equation

$$V_{inv\_av}[k] = V_{g\_av}[k] + L_{fi} \frac{I_L[k+1] - I_L[k]}{T_S} + L_{fg} \frac{I_g[k+1] - I_g[k]}{T_S} \quad (6)$$

According to the dynamic approximation of the LCL filter in [17], the LCL filter acts like an L filter when the LCL filter is properly designed. In this case, the resonance frequency of the filter is higher than controller bandwidth. Therefore, by approximation of $I_g[k] \cong I_L[k]$ and $I_g[k+1] \cong I_L[k+1]$ the predicted current can be obtained as

$$i_g[k+1] = \frac{T_S}{(L_{fi} + L_{fg})} \left(V_{inv\_av}[k] - V_{g\_av}[k] \right) + i_g[k] \quad (7)$$

where $V_{inv\_av}[k]$ and $V_{g\_av}[k]$ are the inverter output voltage and the grid voltage, the average amount over one sampling period. Also, $I_L[k]$ and $I_g[k]$ are the inverter side and the grid side currents at the sampling point of $[k]$.

By assuming the variation of the grid voltage over the switching period is linear [18], the variation of the grid voltage over the switching period of $[k, k+1]$ assume to be equal to the variation over the switching period of $[k-1, k]$ as (8).

$$V_g[\text{k}+1] - V_g[\text{k}] = V_g[\text{k}] - V_g[\text{k}-1] \qquad (8)$$

Therefore, the next sample of the grid voltage can be calculated as

$$V_g[\text{k}+1] = 2V_g[\text{k}] - V_g[\text{k}-1] \qquad (9)$$

by helping a simple linear extrapolation as

$$V_{g\_av}[\text{k}] = \frac{V_g[\text{k}+1] + V_g[\text{k}-1]}{2} \qquad (10)$$

and substituting (9) in (10), the average of the grid voltage over the sampling point of $[k]$ can be calculated as (11).

$$V_{g\_av}[\text{k}] = \frac{3}{2}V_g[\text{k}] - \frac{1}{2}V_g[\text{k}-1] \qquad (11)$$

The same calculation have been done for calculating $V_{g\_av}[k+1]$. In this case, the variation of the grid voltage over the switching period of $[k+1, k+2]$ assume to be equal to the variation over the switching period of $[k, k+1]$.

$$V_g[\text{k}+2] - V_g[\text{k}+1] = V_g[\text{k}+1] - V_g[\text{k}] \qquad (12)$$

$$V_{g\_av}[\text{k}+1] = \frac{V_g[\text{k}+2] + V_g[\text{k}+1]}{2} \qquad (13)$$

$$V_{g\_av}[\text{k}+1] = \frac{5}{2}V_g[\text{k}] - \frac{3}{2}V_g[\text{k}-1] \qquad (14)$$

Therefore, (14) in $\alpha\beta$ frame can be written as

$$V_{g\alpha\_av}[\text{k}+1] = \frac{5}{2}V_{g\alpha}[\text{k}] - \frac{3}{2}V_{g\alpha}[\text{k}-1] \qquad (15)$$

$$V_{g\beta\_av}[\text{k}+1] = \frac{5}{2}V_{g\beta}[\text{k}] - \frac{3}{2}V_{g\beta}[\text{k}-1] \qquad (16)$$

where $V_{g\alpha}[k]$ and $V_{g\beta}[k]$ are the orthogonal components of the grid voltage calculated by an Orthogonal Digital Signal Generator (ODSG) algorithm presented in [19].

C. Switching plan in the proposed MPCC

Switching space vector in a single phase inverter can be defined as

$$S = (S_a + aS_b) \qquad (17)$$

where S_a and S_b are switching states and are determined as

$$S_a = \begin{cases} 1, S_1 = 1 \& S_3 = 0 \\ 0, S_1 = 0 \& S_3 = 1 \end{cases} \qquad S_b = \begin{cases} 1, S_2 = 1 \& S_4 = 0 \\ 0, S_2 = 0 \& S_4 = 1 \end{cases} \qquad (18)$$

where $a = e^{j\pi}$. Finally, the inverter output voltage is defined as equation (19)

$$V_{inv} = SV_{dc} \qquad (19)$$

1) Determining the inverter voltage reference in MPCC.

The switching vectors in the proposed method are given in Fig. 2. The number of vectors in the proposed MPCC can be increased as far as THD reaches within standard zone. Vectors in MPCC are included four basic or real vectors and several virtual vectors.
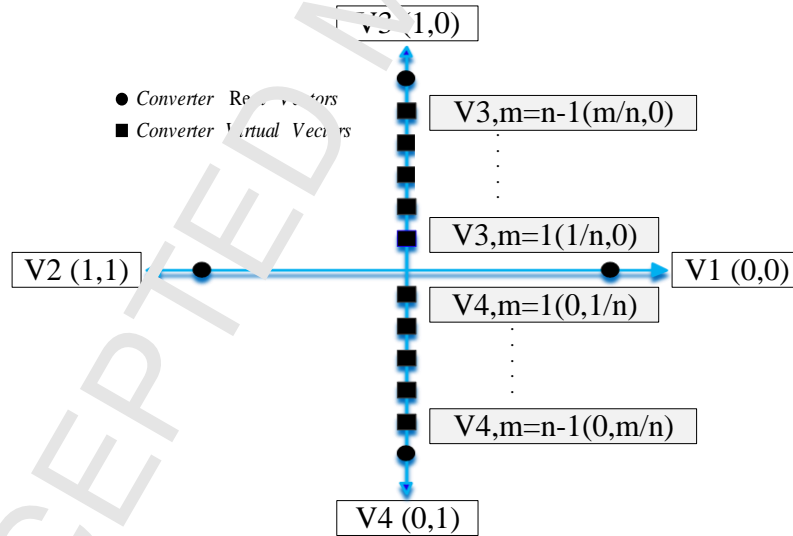

Fig. 2. Voltage vectors generated by single phase inverter with virtual vectors.

2) Determination of the inverter voltage reference ($V_{inv}{}^*$)

The inverter voltage in each switching period can be calculated by

$$V_{in\_av}[k] = \frac{m}{n} V_{dc} \qquad (20)$$

where n is the number of vectors and m varies from 1 to n and implement in (20) to test all amount of $V_{inv-av}[k]$ the in cost function. In this case, all values of V_{inv} in (20) will be placed in (7) and $i_g[k+1]$ is calculated.

Then, $i_g[k + 1]$ is embedded in the cost function (1). Any amount of $i_g[k + 1]$ minimizes the cost function, determines

the inverter voltage reference (V_{inv}^*). Finally, duty cycle time (T_d) for the modulation part is calculated by (21).

$$T_d = \frac{V_{inv}^*}{V_{dc}} T_S \,, \text{or,} \, T_d = \frac{m}{n} T_S \qquad (21)$$

3) Modulation in MPCC

After determination of V_{inv}^* vector, this vector will be applied by switching table given in Table II. In this case, the

selected vector by (20) will be applied during T_d and then the remained time of switching time the zero vector should

be applied, zero time (T_0).

where $$T_0 = T_S - T_d \qquad (22)$$

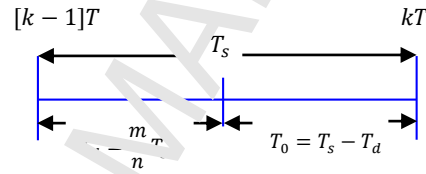One sampling period in the proposed MPCC is shown in Fig. 3.

Fig. 3. Switching time in one sampling period.

The proposed switching table for applying the vectors are listed in Table II.

TABLE II
Switching table for applying vectors in the proposed MPCC

Detected sectors	Selected vector	T_s	
		T_d	T_0
Positive	$V_{3,m}$	V_3 (1 0)	V_1 (0 0)
Negative	$V_{4,m}$	V_4 (0 1)	V_2 (1 1)
Zero	V_1	V_1 (0 0)	
	V_2	V_2 (1 1)	

III. ROBUSTNESS OF THE PROPOSED METHOD

The proposed control method is based on a switching table, where the algorithm searches the best amount of inverter

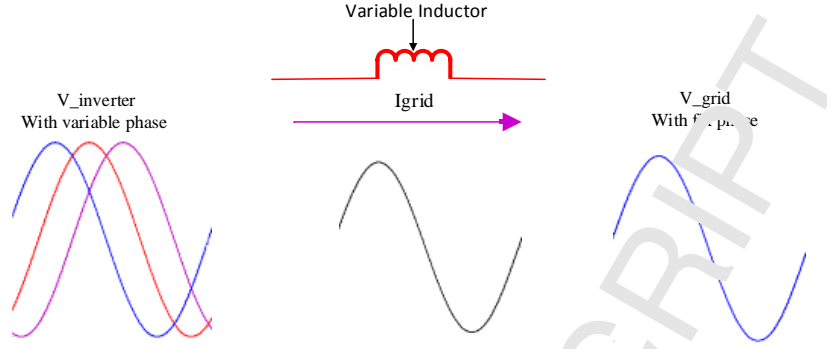voltage to track the current reference.

Fig. 4. The crossing current of the line.

As shown in Fig. 4, when the inductor between the inverter and the grid changes, the inverter should change the phase in the output voltage to compensates this variation effects in order to track the reference current. Otherwise, the grid current shows the error and even instability. Therefore, the grid current can be written as

$$i_{grid} = \frac{V_{inv\_max}\sin(\varphi_{v-inv}) - V_{grid\_max}\sin(\varphi_{v-grid})}{X_L} \tag{23}$$

where $V_{inv\_max}\sin(\varphi_{V-inv})$ is the inverter output voltage, $V_{grid\_max}\sin(\varphi_{V-grid})$ is the grid voltage and X_L is the inductor impedance between the inverter and the grid. In the proposed control method, the algorithm searches to find the best amount for the inverter voltage to track the reference. Therefore, if the grid impedance varies, the selected inverter voltage average is varied to have a stable operation. In this case, the first part ($\frac{Ts}{L_{fi}+L_{fg}}$) in (7) is fix when the inductor L_{fg} changes by grid impedance variations and the new amount of L_{gf} can't update in $\frac{Ts}{L_{fi}+L_{fg}}$. However, as the algorithm is based on switching table and cost function, this error will be compensated with another vector of the inverter voltage. In fact, the variation of L_{fg} cannot make an error for the controller. For example, when the L_g changes, the measured current $i_g[k]$ is changed in (7) and the controller has to change the inverter output voltage ($V_{inv}[k]$) in order to minimize the cost function as Fig. 5. Therefore, the robustness of proposed method is due to the cost function and the switching table nature.
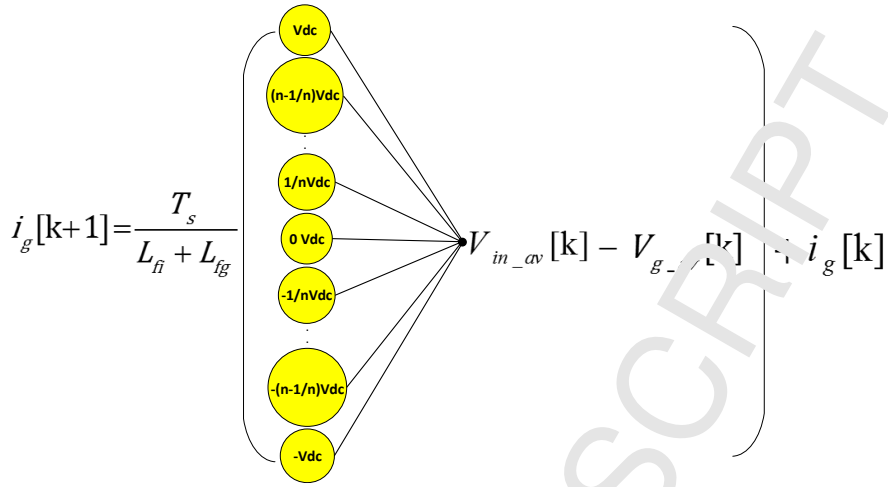
$$i_g[k+1] = \frac{T_s}{L_{fi} + L_{fg}} \left(V_{in\_av}[k] - V_{g\_}[k] \right) + i_g[k]$$

Fig. 5. The principle of the predicted current equation.

Fig. 6 shows the inverter voltage references V_{inv}^* created by the proposed MPCC controller for different L_g. The grid impedance (L_g) changes from 1 mH to 10 mH and the inverter voltage reference has been recorded. As it is shown, the proposed MPCC changes the phase of the inverter voltage reference to control the grid current when the grid impedance changes. This phase change is carried out by selecting the best vector in order to minimize the error of the current reference and the grid current based on the cost function.
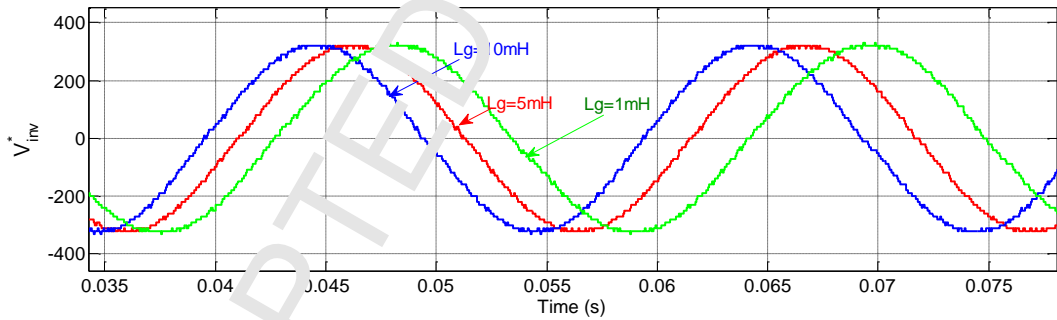

Fig. 6. The inverter voltage reference under different L_g.

The control block diagram of the proposed MPCC is given in Fig. 7.
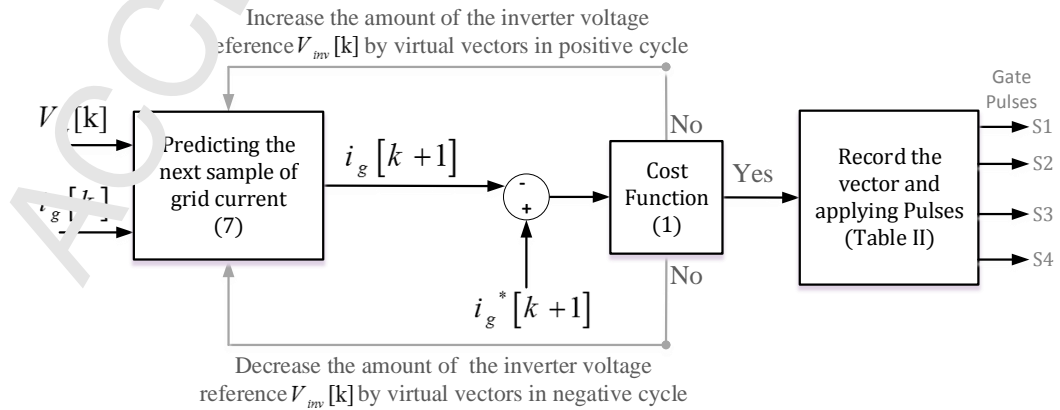

Fig. 7. The control block diagram of the proposed MPCC.

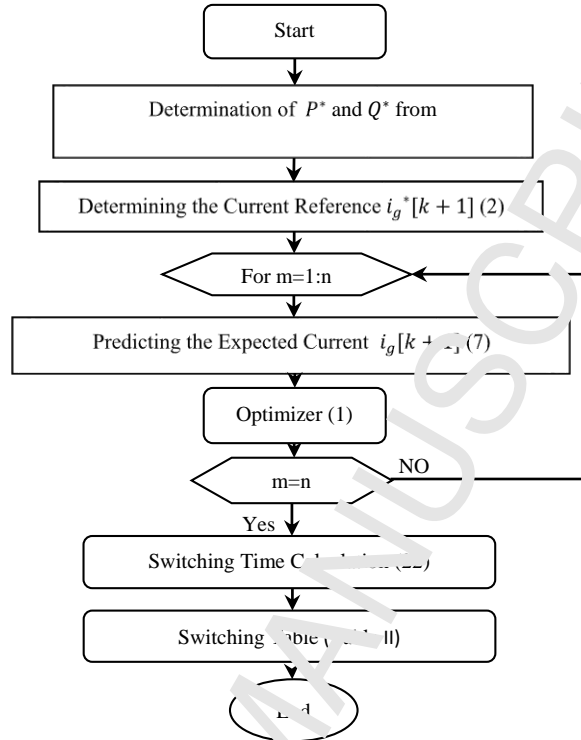The control flowchart of the proposed controller is shown in Fig. 8.

Fig. 8. The control flowchart of the proposed MPC.

IV. SIMULATION RESULTS

The performance of the proposed control have been carried out in Matlab/Simulink using PLECS blocks. The parameters of the system for both simulation and experiments are listed in Table III. In order to evaluate the performance of the proposed controller, the results have been compared with a classical PR controller when the PR controller is designed in a proper condition, phase margin of 45 degrees. In this case, some case studies are conducted.

TABLE III

Simulation and experimental parameters

Description	Value
Grid Frequency	$\omega = 2\pi \times 50$ rad/s
Grid Voltage	$V_g = 230$ V
maximum Power	$P_n = 1$ kW
DC-bus voltage	$V_{dc} = 400$ V
Switching Frequency	$F_{sw} = 10$ kHz
LCL-Filter capacitance	$C = 2.35\mu F$
Inverter Side Inductance	Lfi = 3.6 mH
Grid Side Inductance	Lfg = 708μH

A. Operating in Normal condition

In this case study, in order to evaluate both controllers in normal condition ($L_g = 1\ mH$) two steps in active and reactive power have been done and the results are shown in Fig. 9. As it seen in Fig. 9, the proposed controller like the PR controller precisely tracked the power references.
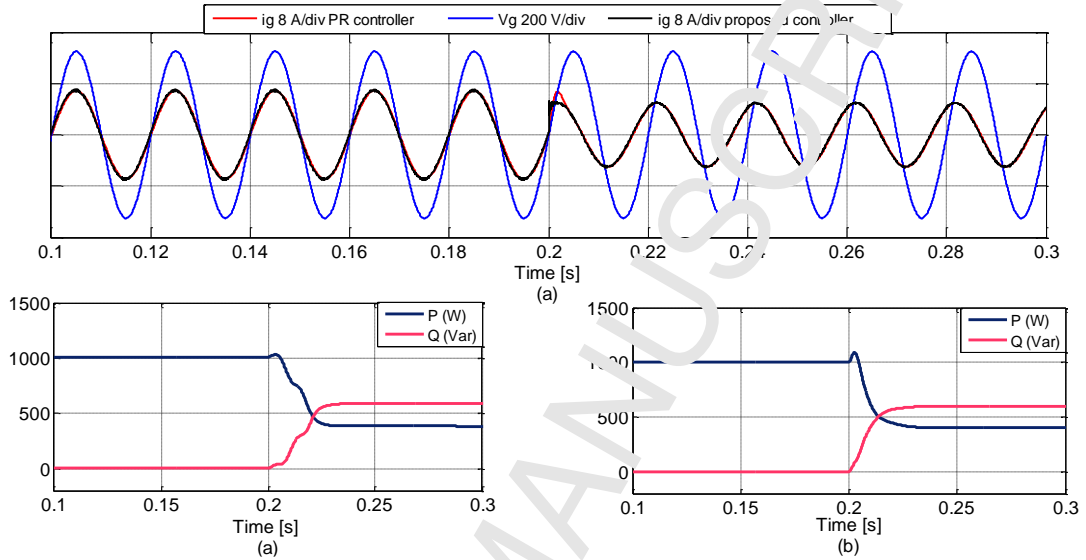

Fig. 9. Grid voltage and current in injecting active and reactive power: (a) proposed MPCC, (b) PR controller.

B. Operating condition in grid impedance variation

Due to Table III, the amount of the grid side inductor is 1mH and due to the grid impedance is series with this inductor, the grid impedance (L_g) is changed from 1 mH to 5 mH. Fig. 10 shows the grid current for the grid impedance variation from 1 mH to 5 mH. As shown in Fig. 10, when $L_g = 1\ mH$ (the intended amount for designing PR parameters) two controllers exactly track the current reference without any error. When the grid impedance increase, 3 mH, 4 mH, and 5 mH, the PR controller has not an acceptable response and it is unstable for 5 mH, but the proposed MPCC remains stable without any oscillations against the grid impedance variations.
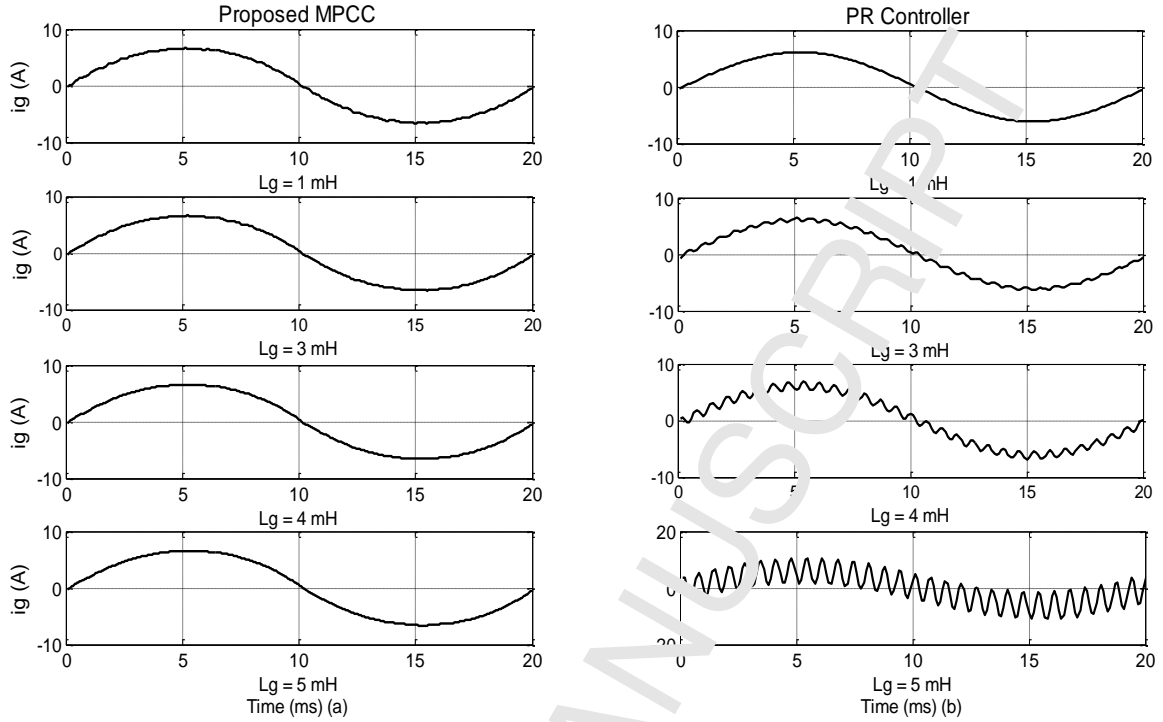
Fig. 10. Grid current with variation of L_g from $1\ mH$ to $5\ nH$: (a) proposed MPCC, (b) PR controller.

C. Operating condition in filter parameter variation

In order to more evaluate the robustness of the proposed controller the ratio of inverter side to grid side has been changed (both $L_{gi} > L_{gf}$ and $L_{gi} < L_{gf}$) and the injected current recorded as Fig. 11. As it is shown in Fig. 11, the injected current by the proposed controller is without any distortion and instability in all condition.
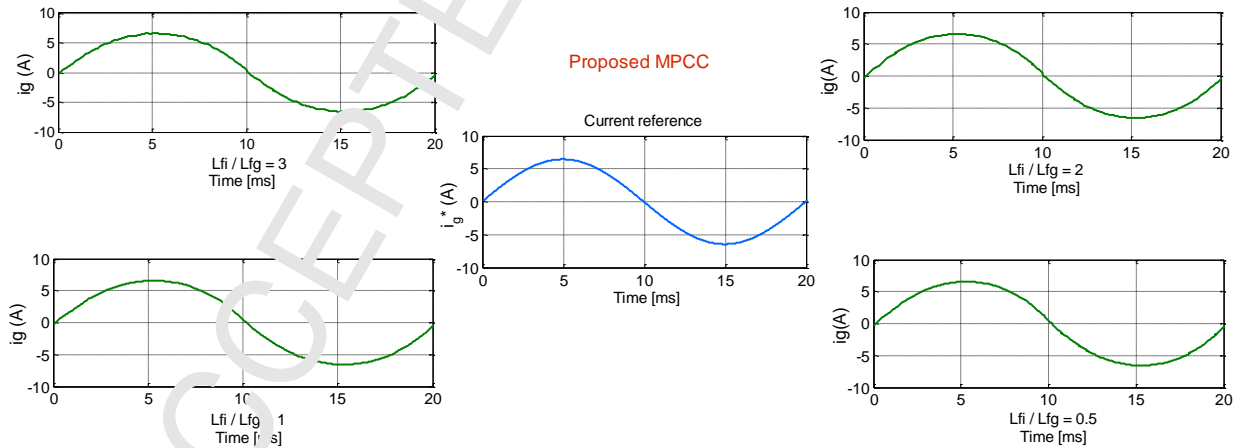

Fig. 11. Injected current by the proposed controller in different ratio of inverter side inductor and grid side inductor.

D. Operating condition in tracking step reference

In this case study, two controllers are forced to track a current reference when a step occurred in this reference. Fig. 12 and Fig. 13 show the grid current for a step response reference operation from 5 A peak to 10 A peak for two conditions, $L_g = 1\ mH$ and $L_g = 2\ mH$. As it can be seen in Fig. 12, the proposed MPCC has a faster dynamic response and lower overshoot even for a normal condition compared with the PR controller.
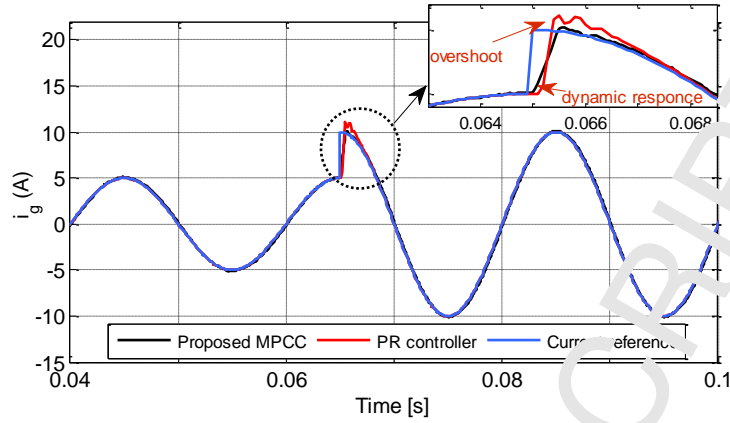
Fig. 12. Step response reference and grid current with the step from 5 A to 10 A, in normal operation $L_g = 1$ mH: (a) proposed MPCC, (b) PR controller.

In Fig. 13, when the grid branch inductance is increased to $2\ mH$ ($L_g = 2\ mH$), by adding a series inductor to the grid side filter inductor, the grid current oscillates for two cycles after the step instant, while the proposed MPCC does not show any distortion after the step instant.
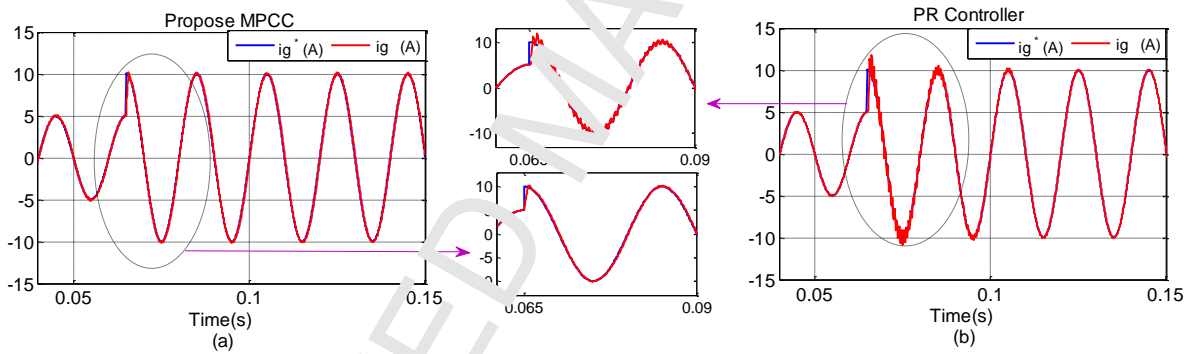

Fig. 13. Step response reference and grid current with the step from 5 A to 10 A in $L_g = 2$ mH: (a) proposed MPCC, (b) PR controller.

E. Short circuit operation

In this case, a current reference 5 A is forced to track by both controllers and a short circuit occurs in the grid voltage during injection current process. Fig. 14 shows the performance of both controllers in this operation. As it can be seen from Fig. 14, in contrast to the PR controller, the proposed controller at the grid fault and the clean fault time and has a better performance without any oscillation.
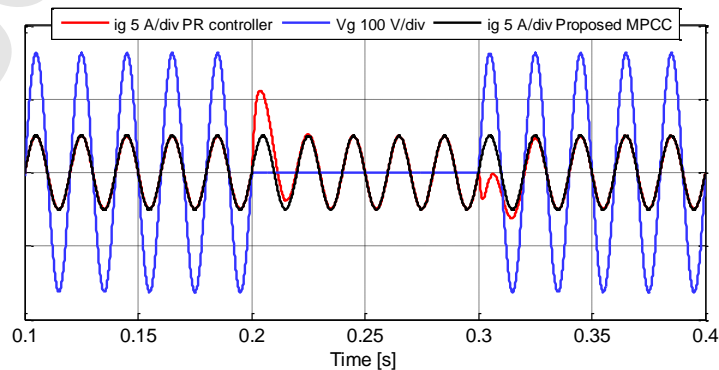

Fig. 14. The performance of both controllers in short circuit operation when L_g is 1 mH, (a) Proposed MPCC, (b) PR Controller.

V. EXPERIMENTAL RESULTS

The same case studies used for the simulation tests have also been implemented by the experimental setup. A single-phase Danfoss inverter is connected to the grid through an LCL filter. The inverter is controlled by dSPACE 1007. DC link is supported by an adjustable DC/DC converter. The experimental configuration is shown in Fig. 15. Fig. 16 shows the results for both controllers when the reference of the active and reactive power change from 1000 to 400 W and 0 to 600 Var. This case is done for $L_g = 1\ mH$. Fig. 17 shows the grid current against the grid impedance variations for two controllers. In this case, the grid impedance changes from $1\ mH$ to $3\ mH$ by adding a series inductor to the grid side filter inductor. As it is seen in Fig. 17, the PR controller is going to be unstable when the grid impedance is increased. On the other hand, the proposed controller is stable against the variation of grid impedance. Finally, Fig. 18 shows the grid current when a step response occurs in the current reference and L_g is $1\ mH$ for both controllers. As shown in Fig. 18, in contrast to the proposed controller, the PR controller creates a distortion when the step current is activated.
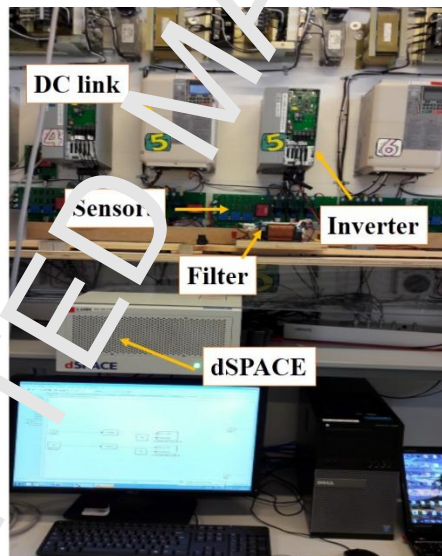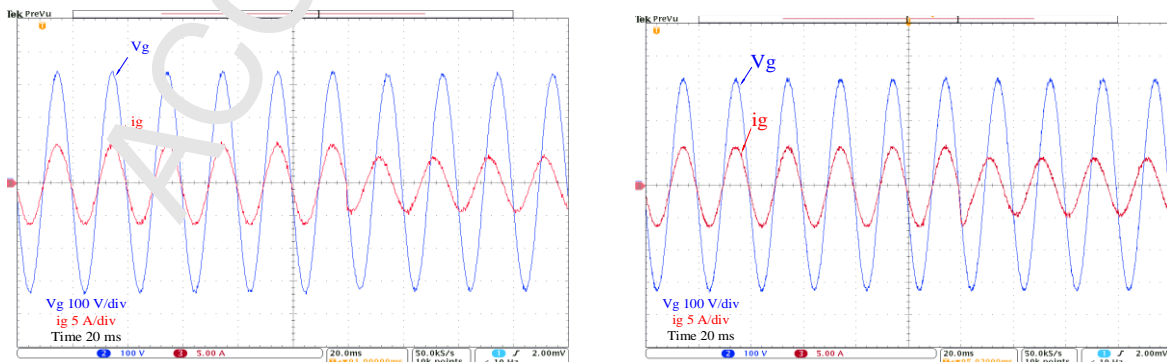

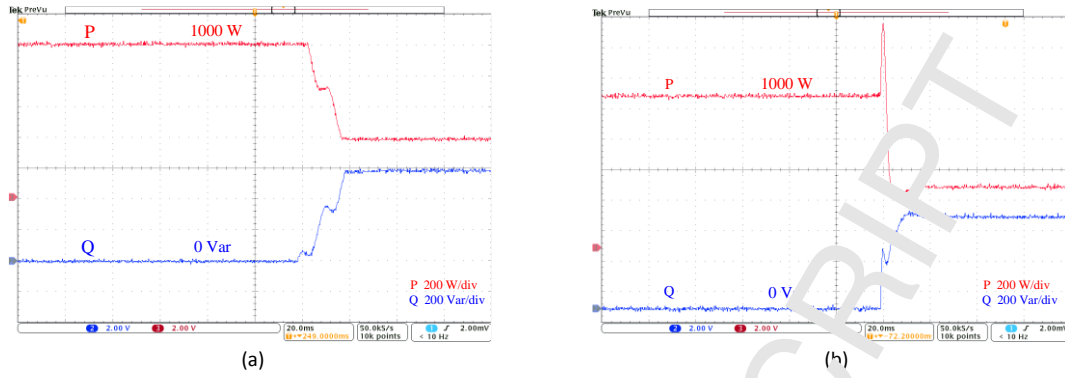Fig. 15. Experimental setup configuration.

Fig. 15. Grid voltage and current in PQ operation: (a) the proposed controller, (b) PR controller.

(a)   (b)   (c)
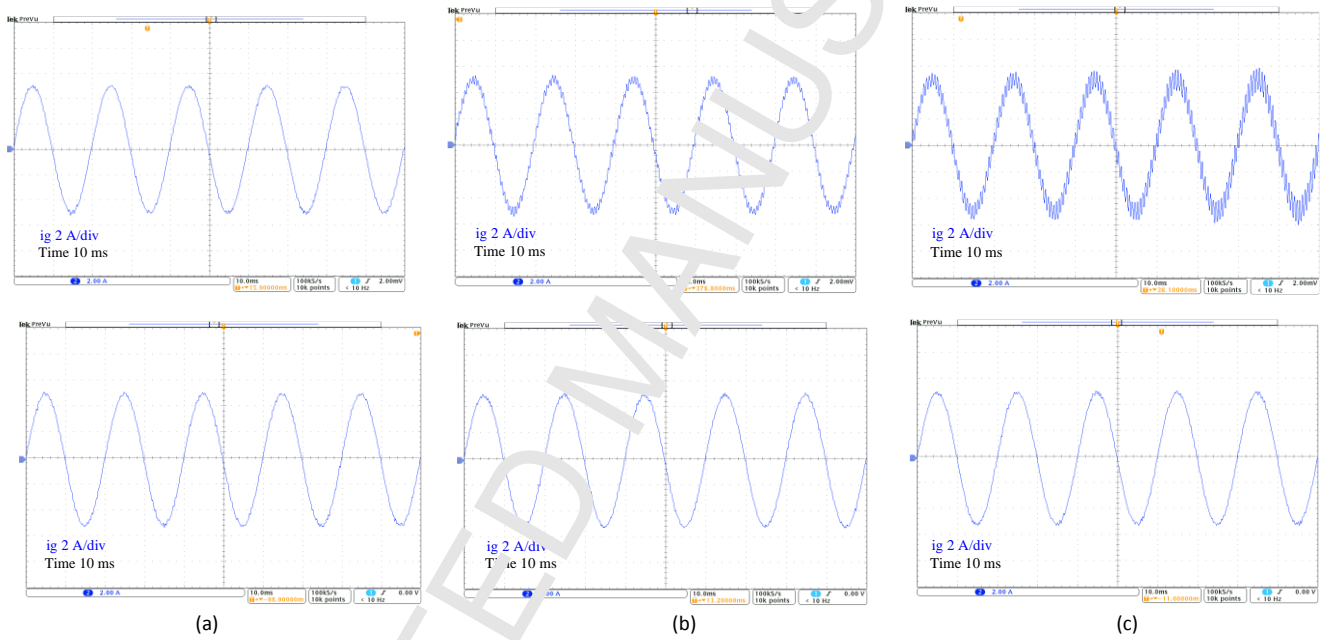
Fig. 16. Grid current in grid impedance variation (top) PR controller, (bottom) the proposed controller, (a) $L_{grid} = 0\ mH$, (b) $L_{grid} = 1\ mH$ (c) $L_{grid} = 2\ mH$.

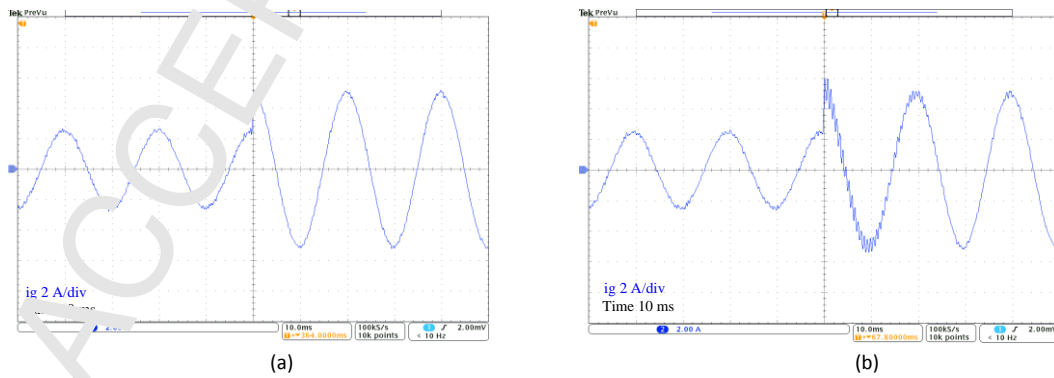

(a)   (b)

Fig. 17. Grid current in step response operation with $L_{grid} =\ 2\ m\ H$: (a) the proposed controller, (b) PR controller.

VI. CONCLUSION

In this paper, an MPCC current controller presented, where it is simple and does not need any parameter tuning. In the proposed method, the final switching pulse is determined by a cost function. In order to increase the accuracy and adaptability of the proposed MPCC, some virtual vectors have been applied by a switching table. Against the multi-loop controllers, which are sensitive to variation of the system parameters, the proposed MPCC controller is fully adaptive and acts based on the real time conditions of the system. Some case study have been done to prove the effectiveness of the proposed controller in different conditions. In this case, the results show: when the grid is in normal condition, without variation in grid impedance, the proposed controller has even more dynamic response and lower overshoot in tracking the step reference. When a fault occurred in the grid voltage during current injection, the injected current by the PR controller makes some distortion in fault time and clean fault time while the injected current by the proposed controller is without distortion. Also, when the grid impedance varies, in contrast the PR controller, the proposed controller remains stable. In future, due to the simplicity, robustness and high dynamic characteristic of MPC based controllers, these controllers can be a promising controller for grid-connected single-phase inverters with the LCL filter at the output like PV inverters. Therefore, these controllers can be engaged to control MPPT in DC/DC stage, DC link ripple reduction and inverter current control in a PV systems.

References

[1] Mohamed Y. Suppression of low and high-frequency instabilities and grid-induced disturbances in distributed generation inverters. IEEE Trans Power Electron 2011;26(12):3790–3803.

[2] Xingang S, Ramezani M, Sun Y, Won H. A novel direct-current vector control technique for single-phase inverter with L, LC and LCL filters. Electr Power Syst Res 2015;125:235-244.

[3] Lindgren M, Svensson J. Control of a voltage-source converter connected to the grid through an LCL-filter-application to active filtering. IEEE PESC 1998;1:229–235.

[4] Park S, Chen C, Lai J, Moon S. Admittance compensation in current loop control for a grid-tie LCL fuel cell inverter. IEEE Tran Power Electron 2008;23(4):1716-1723.

[5] Bierhoff M, Fuchs F. Active damping for three-phase PWM rectifiers with high-order line-side filters. IEEE Trans Ind Electron 2009;56(2):371–379.

[6] Dannehl J, Wessels C, Wilhelm F. Limitations of voltage-oriented PI current control of grid-connected PWM rectifiers with LCL filters. IEEE Trans Ind Electron 2009;56(2):380 – 388.

[7] Xu J, Xie S, Huang L, Ji L. Design of LCL-filter considering the control impact for grid-connected inverter with one current feedback only. IET Power Electron 2017;10(11):1324 – 1332.

[8] Liserre M, Blaabjerg F, Hansen S. Design and control of an LCL-filter-based three-phase active rectifier. IEEE Trans Ind Appl 2005;41(5):1281 – 1291.

[9] Alemi P, Bae C, Lee D. Resonance suppression based on PR control for single-phase grid-connected inverters with LLCL filters. IEEE JESTPE 2016;4(2):459-467.

[10] Alzola R, Liserre M, Blaabjerg F, Ordonez M, Kerekes T. A self-commissioning notch filter for active damping in a three-phase LCL -filter-based grid-tie converter. IEEE Trans Power Electron 2014,29(2):6754-6761.

[11] Liserre M, Dell'Aquila A, Blaabjerg F. Genetic algorithm-based design of the active damping for an LCL-filter three-phase active rectifier. IEEE Trans Power Electron 2004;19(1):76-86.

[12] Dannehl J, Liserre M, Fuchs F. Filter-based active damping of voltage source converters with LCL filter. IEEE Trans Ind Electron 2011;58(8):3623-3633.

[13] Yang S, Peng Q, Qian Z. A robust control scheme for grid-connected voltage-source inverters. IEEE Trans Ind Electron 2011;58(1):202-212.

[14] Li X, Wu X, Geng Y, Yuan X, Xia C, Zhang X. Wide damping region for LCL-type grid-connected inverter with an improved capacitor-current-feedback method. IEEE Trans Power Electron 2015;30(9):5247-5259.

[15] Chai S, Wang L, Rogers E. Model predictive control of a permanent magnet synchronous motor with experimental validation. Control Eng Pract 2013;21 (11):1584–92.

[16] Vesely V, Rosinova D, Foltin M. Robust model predictive control design with input constraints. ISA Trans 2010;49:114–20.

[17] Castello J, Garcia-Gil R, Garcera G, Figueres E. A adaptive robust predictive current control for three-phase grid-connected inverters. IEEE Trans Ind Electron 2011;58(8):3537–3546.

[18] Holmes D, Martin D. Implementation of a direct digital predictive current controller for single and three phase voltage source inverters. Ind Appl Conf 1996:906-913.

[19] Choi J, Kim Y, Kim H. Digital PLL control for single-phase photovoltaic system. IEE Proc - Electr Power Appl 2006;153(1):40-46.